

Accepted Manuscript

Network analysis and mechanisms of action of Chinese herb-related natural compounds in lung cancer cells

Ying-Ju Lin , Wen-Miin Liang , Chao-Jung Chen , Hsinyi Tsang , Jian-Shiun Chiou , Xiang Liu , Chi-Fung Cheng , Ting-Hsu Lin , Chiu-Chu Liao , Shao-Mei Huang , Jianxin Chen , Fuu-Jen Tsai , Te-Mao Li

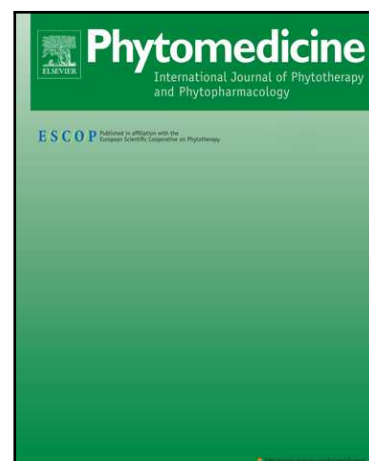
PII: S0944-7113(19)30063-7
DOI: <https://doi.org/10.1016/j.phymed.2019.152893>
Article Number: 152893
Reference: PHYMED 152893

To appear in: *Phytomedicine*

Received date: 9 January 2019
Revised date: 9 March 2019
Accepted date: 12 March 2019

Please cite this article as: Ying-Ju Lin , Wen-Miin Liang , Chao-Jung Chen , Hsinyi Tsang , Jian-Shiun Chiou , Xiang Liu , Chi-Fung Cheng , Ting-Hsu Lin , Chiu-Chu Liao , Shao-Mei Huang , Jianxin Chen , Fuu-Jen Tsai , Te-Mao Li , Network analysis and mechanisms of action of Chinese herb-related natural compounds in lung cancer cells, *Phytomedicine* (2019), doi: <https://doi.org/10.1016/j.phymed.2019.152893>

This is a PDF file of an unedited manuscript that has been accepted for publication. As a service to our customers we are providing this early version of the manuscript. The manuscript will undergo copyediting, typesetting, and review of the resulting proof before it is published in its final form. Please note that during the production process errors may be discovered which could affect the content, and all legal disclaimers that apply to the journal pertain.



Network analysis and mechanisms of action of Chinese herb-related natural compounds in lung cancer cells

Ying-Ju Lin^{a,b}, Wen-Miin Liang^c, Chao-Jung Chen^{b,d}, Hsinyi Tsang^{e,f}, Jian-Shiun Chiou^c, Xiang Liu^e,
Chi-Fung Cheng^{b,c}, Ting-Hsu Lin^b, Chiu-Chu Liao^b, Shao-Mei Huang^b, Jianxin Chen^g, Fuu-Jen
Tsai^{a,b,h,*}, Te-Mao Li^{a,*}

^aSchool of Chinese Medicine, China Medical University, Taichung, Taiwan

^bGenetic Center, Proteomics Core Laboratory, Department of Medical Research, China Medical University Hospital, Taichung, Taiwan

^cGraduate Institute of Biostatistics, School of Public Health, China Medical University, Taichung, Taiwan

^dGraduate Institute of Integrated Medicine, China Medical University, Taichung, Taiwan

^eCenter for Biomedical Informatics and Information Technology, National Cancer Institute, National Institutes of Health, Gaithersburg, MD, USA

^fAttain, LLC, McClean, Virginia, USA

^gBeijing University of Chinese Medicine, ChaoYang District, Beijing, China

^hDepartment of Biotechnology and Bioinformatics, Asia University, Taichung, Taiwan

Ying-Ju Lin, Wen-Miin Liang, and Chao-Jung Chen contributed equally to this work.

*Corresponding authors at: School of Chinese Medicine, China Medical University, Taichung, Taiwan. Tel.: +886 4 22053366; fax: +886 4 22053366.

E-mail addresses: d0704@mail.cmuh.org.tw (F.J. Tsai), leedemaw@mail.cmu.edu.tw (T.M. Li).

ABSTRACT

Background: Chinese herbal medicines (CHMs) are a resource of natural compounds (ingredients) and their potential chemical derivatives with anticancer properties, some of which are already in clinical use. Bei-Mu (BM), Jie-Geng (JG), and Mai-Men-Dong-Tang (MMDT) are important CHMs prescribed for patients with lung cancer that have improved the survival rate.

Hypothesis/Purpose: The aim of this study was to systemically investigate the mechanisms of action of these CHM products in lung cancer cells.

Methods: We used a network pharmacology approach to study CHM product-related natural compounds and their lung cancer targets. In addition, the underlying anti-lung cancer effects of the natural compounds on apoptosis, cell cycle progression, autophagy, and the expression of related proteins was investigated *in vitro*.

Results: Ingredient–lung cancer target network analysis identified 20 natural compounds. Three of these compounds, ursolic acid, 2-(3R)-8,8-dimethyl-3,4-dihydro-2H-pyrano(6,5-f)chromen-3-yl)-5-methoxyphenol, and licochalcone A, inhibited the proliferation of A549 lung cancer cells in a dose-dependent manner. Signal pathway analyses suggested that these three ingredients may target cellular apoptosis, anti-apoptosis, and cell cycle-related proteins. These three ingredients induced apoptosis through the regulation of the expression of apoptotic and anti-apoptotic proteins, including B-cell lymphoma-2 and full-length and cleaved poly(ADP-ribose) polymerase proteins. They also induced cell cycle arrest in S and G2/M phases and autophagy in A549 cells.

Conclusion: The pharmacological mechanisms of ingredients from MMDT on lung cancer may be strongly associated with their modulatory effects on apoptosis, autophagy, cell cycle progression, and cell proliferation.

Keywords: Lung cancer, Chinese herbal medicine, natural compound, network analysis, apoptosis

Abbreviations: BM, Bei-Mu; BX, Ban-Xia; CHM, Chinese herbal medicine; DZ, Da-Zao; FITC, fluorescein isothiocyanate; GC, Gan-Cao; GDC, Genomic Data Commons; IPA, Ingenuity Pathway Analysis; JG, Jie-Geng; KEGG, Kyoto Encyclopedia of Genes and Genomes; MMDT, Mai-Men-Dong-Tang; PBS, phosphate-buffered saline; PI, propidium iodide; RS, Ren-Shen; TCM, traditional Chinese medicine; TCMSp, Traditional Chinese Medicine Systems Pharmacology database and analysis platform; WHO, World Health Organization

ACCEPTED MANUSCRIPT

Introduction

Cancer is a leading cause of mortality worldwide. According to a World Health Organization (WHO) report, approximately 8.8 million deaths were associated with cancers in 2015 (<http://www.who.int/mediacentre/factsheets/fs297/en/>). The mortality rate of patients with lung cancer is noteworthy, with 1.69 million deaths reported. In Taiwan, lung cancer is the most common cause of cancer-related death. Survival of patients with lung cancer is poor and ranges from 6% to 18% (Chiang et al., 2016; Wang et al., 2013a).

Chinese herbal medicines (CHMs) are an important part of the healthcare system in Taiwan (Lee et al., 2010). Taiwanese people choose western medicine, CHM, or both. The pattern of use of CHMs has been investigated for diseases such as childhood asthma (Huang et al., 2013), breast cancer (Hsu et al., 2015), and diabetes (Tsai et al., 2017). The National Health Insurance Research Database provides a platform to explore the utilization and therapeutic effects of Chinese herbal therapies prescribed by traditional Chinese medicine (TCM) doctors in Taiwan. To better understand the role of CHM as an adjunctive therapy in patients with lung cancer, we investigated the demographic characteristics, overall survival, and CHM-prescribing patterns for these patients using data retrieved from a population-based database. Our findings showed that CHM users had a high cumulative survival probability among patients with lung cancer (Li et al., 2018a). We obtained detailed data on the most commonly used prescription patterns of herbal formulae, single herbs, and their combinations among CHM users. Bei-Mu (BM), Jie-Geng (JG), and Mai-Men-Dong-Tang (MMDT)

were important CHM prescriptions for patients with lung cancer and were associated with good survival rates.

Cancer cell apoptosis is characterized by mitochondrial outer membrane permeabilization and the release of cell death factors, including cytochrome c, into the cytoplasm, which leads to caspase activation and apoptosis (Liang et al., 2012). Studies have shown that CHMs induce cancer cell apoptosis (Lu, 2016; Niu et al., 2011; Zhang et al., 2012; Zhong et al., 2013) and are a resource of natural compounds and their potential chemical derivatives with anticancer properties, some of which are already in clinical use (Bailon-Moscoso et al., 2017; Venkata Sairam et al., 2016). In this study, we aimed to investigate the mechanisms underlying the effects of CHM product-related natural compounds on lung cancer cell apoptosis using network analysis and *in vitro* functional studies.

Materials and methods

Ingredients (natural compounds) in BM, JG, and MMDT, and their targets

Data on BM, JG, and MMDT were obtained from TCMSP (<http://lsp.nwu.edu.cn/> updated on May, 2014) (Ru et al., 2014), TCM-MESH (<http://mesh.tcm.microbioinformatics.org/> updated on April, 2017) (Zhang et al., 2017), and SymMap (<http://www.symmap.org/search/> updated on October, 2018) (Wu et al., 2019) (Table 1 and Table S1).

For BM, seven ingredients were found in at least two of the three CHM databases (Table S2). These seven ingredients had a total of 44 targets, and ingredient–target interaction data from the

three CHM databases are presented in Table S2. For JG, nine ingredients were found in at least two of the three CHM databases (Table S3), with a total of 130 targets. Ingredient–target interaction data from the three CHM databases are presented in Table S3. MMDT was composed of five single herbs, Ban-Xia (BX), Gan-Cao (GC), Ren-Shen (RS), Da-Zao (DZ), and Tian-Dong (TD). For RS, 41 ingredients were found in at least two of the three CHM databases (Table S4). These 41 ingredients had a total of 263 targets, and ingredient–target interaction data from the three CHM databases are presented in Table S4. For DZ, 41 ingredients were found in at least two of the three CHM databases (Table S5), with a total of 390 targets. Ingredient–target interaction data from the three CHM databases are presented in Table S5. For BX, 40 ingredients were found in at least two of the three CHM databases (Table S6). These 40 ingredients had a total of 365 targets, and ingredient–target interaction data from the three CHM databases are presented in Table S6. For GC, 88 ingredients were found at least two of the three CHM databases (Table S7), with a total of 307 targets. Ingredient–target interaction data from the three CHM databases are presented in Table S7. For TD, 15 ingredients were found in at least two of the three CHM databases (Table S8). These 88 ingredients had a total of 217 targets, and ingredient–target interaction data from the three CHM databases are presented in Table S8.

Lung cancer targets obtained from Ingenuity Pathway Analysis (IPA) and Genomic Data

Commons (GDC) resources

Human lung cancer targets were retrieved from <https://www.qiagenbioinformatics.com/products/ingenuity-pathway-analysis/>. When using the search term “lung cancer,” 2,628 lung cancer targets were retrieved, and when using the search term “lung cancer and protein,” 837 lung cancer targets were found (Table S9). In addition, human lung cancer targets were retrieved from the GDC Data Portal, National Cancer Institute, National Institutes of Health (<https://portal.gdc.cancer.gov/>). In total, 570 lung cancer targets were retrieved from this database (Table S9). In this study, we used 2,628 human lung cancer targets with their Entrez Gene ID as lung cancer target resource.

Network analysis

Network analysis was performed as follows. (1) Networks of ingredient–lung cancer target and ingredient–target were plotted using Cytoscape (<https://cytoscape.org/>, version 3.7.0) (Shannon et al., 2003). Ingredient–target interaction data from the three CHM databases were used to plot networks (BM, Table S2 and Fig. S1; JG, Table S3 and Fig. S2; MMDT Tables S4-S8 and Fig. S3. For BM, JG, and MMDT, ingredient–lung cancer target interaction data from the three CHM databases were used to plot a network (Tables S2–S9 and Fig. 1). (2) A putative gene–gene interaction network of the obtained lung cancer targets of the natural compounds was constructed using IPA software

(<https://www.qiagenbioinformatics.com/products/ingenuity-pathway-analysis/>) (Fig. S4 and Table S8). (3) Putative signaling pathways of the obtained lung cancer targets of three natural compounds, ursolic acid, 2-[(3R)-8,8-dimethyl-3,4-dihydro-2H-pyrano[6,5-f]chromen-3-yl]-5-methoxyphenol, and licochalcone A, were mapped to “pathways in cancer” using the Kyoto Encyclopedia of Genes and Genomes (KEGG) website (<https://www.genome.jp/kegg/>) (Fig. S6 and Table S13).

Cells

The human non-small cell lung cancer cell line A549 was used in this study. Cells were cultured in Dulbecco’s modified Eagle’s medium supplemented with 10% heat inactivated fetal bovine serum and 1% antibiotic at 37°C in a 5% CO₂ incubator.

Chemical compounds

Ursolic acid (catalog number: S2370; purity: 99.8%), baicalein (catalog number: S2268; purity: 98.5%), luteolin (catalog number: S2320; purity: 99.1%), and acacetin (catalog number: S5318; purity: 99.9%) were purchased from Selleck Chemicals (Houston, TX, USA). Beta-elemene (catalog number: 19641; purity: ≥95.0 %) and naringenin (catalog number: 14173; purity: ≥98.0%) were purchased from Cayman Chemical (Ann Arbor, MI, USA). Quercetin (catalog number: ab120247; purity: >99.0%) and glabridin (2-[(3R)-8,8-dimethyl-3,4-dihydro-2H-pyrano[6,5-f]chromen-3-yl]-5-methoxyphenol; catalog number: ab143625; purity: >98.0%) were purchased from Abcam (Cambridge, MA, USA). Beta-sitosterol (catalog number: S9889; purity: ≥96.0%) and cisplatin (catalog number: P4394; purity: 100%) were purchased from Sigma-Aldrich (St. Louis, MO, USA). Licochalcone A (catalog number: CFN99575; purity: >98.0%), 1-methoxyphaseollidin (catalog number: CFN96878; purity: ≥98.0%), (L)-alpha-terpineol (catalog number: CFN80110; purity: ≥98.0%), kaempferol (catalog

number: CFN98838; purity: >98.0%), palmitic acid (catalog number: CFN99716; purity: \geq 98.0%), berberine (catalog number: CFN98049; purity: \geq 98.0%), and formononetin (catalog number: CFN99962; purity: >98.0%) were purchased from ChemFaces Biochemical (Wuhan, Hubei, China). 5-Methyl-7-methoxyisoflavone (7-methoxy-2-methyl isoflavone; catalog number: 00013612; purity: 98.8%) was purchased from ChromaDex (Irvine, CA, USA). Paclitaxel (Phyxol[®], a clinically available paclitaxel formulation containing 6 mg paclitaxel, 527 mg Cremaphor EL, and 47.7% (v/v) alcohol/mL) was obtained from Sinphar Pharmaceutical (Taipei, Taiwan). Topotecan (Hycamtin[®], Injection, a clinically available topotecan, 4MG) was obtained from Novartis Pharmaceuticals (East Hanover, NJ, USA).

Cell viability assay

A549 cells were seeded in 96-well plates (1×10^2 cells/well) and allowed to settle for 12 h before treatment. The cells were treated with natural compounds (10, 50, and 100 μ M for each natural compound) for 24 h in an incubator at 37°C with 5% CO₂ (Shi et al., 2016). Cell viability was determined using a 4-[3-(4-iodophenyl)-2-(4-nitrophenyl)-2H-5-tetrazolio]-1,3-benzene disulfonate (WST-1) assay (Roche, Indianapolis), following the manufacturer's instructions (Table 1 and Fig. S4). Cell survival rates were calculated as the ratio of the optical density at a wavelength of 450 nm (OD₄₅₀) of treated cells (10, 50, and 100 μ M for each natural compound) to that of non-treated cells. Each concentration was tested in quadruplicate, and representative results of three independent experiments are shown.

Cell apoptosis analysis

A549 cells were seeded in six-well plates and incubated for 12 h before treatment. The cells were then treated with ursolic acid, 2-[(3R)-8,8-dimethyl-3,4-dihydro-2H-pyrano[6,5-f]chromen-3-yl]-5-methoxyphenol, or licochalcone A (20, 40, and 80 μ M for each natural compound) for 24 h in an incubator at 37°C with 5% CO₂. Then, the cells were harvested, washed twice with ice-cold phosphate-buffered saline (PBS), incubated with Annexin V-fluorescein isothiocyanate (FITC) for 10 min, and treated with propidium iodide (PI) for 5 min. The apoptosis rate was evaluated using a FLOW-TUNEL assay (APO-DIRECT™ Kit (cat no. 556381), FACSCalibur, BD Biosciences, CA, USA). Apoptotic cells were calculated as the sum of the percentages in the second and fourth quadrants. Each concentration was tested in quadruplicate, and representative results of three independent experiments are shown.

Cell cycle analysis

A549 cells were seeded in six-well plates and incubated for 12 h before treatment. The cells were treated with ursolic acid, 2-[(3R)-8,8-dimethyl-3,4-dihydro-2H-pyrano[6,5-f]chromen-3-yl]-5-methoxyphenol, or licochalcone A (20, 40, and 80 μ M for each natural compound) for 24 h in 5% CO₂ incubator at 37°C. Following treatment, the cells were collected and fixed with 75% ice-cold ethanol and stored at -20°C for 1 h. Cells were harvested by centrifugation, washed twice with ice-cold PBS, and incubated with PI at 4°C for 20 min. Cell cycle evaluation was performed using a cell cycle assay (Propidium Iodide Flow Cytometry Kit [ab139418], FACSCalibur; BD Biosciences, CA, USA). The cell fractions in sub-G₀, G₀/G₁, S, and G₂/M phases were used for statistical analysis with FlowJo 7.6 software (TreeStar, San Carlos, CA, USA). Each concentration was tested in quadruplicate, and representative results of three independent experiments are shown.

Western blot analysis

A549 cells were seeded in six-well plates for 12 h before treatment. The cells were treated with ursolic acid, 2-[(3R)-8,8-dimethyl-3,4-dihydro-2H-pyrano[6,5-f]chromen-3-yl]-5-methoxyphenol, or licochalcone A (20, 40, and 80 μ M for each natural compound) for 24 h in an incubator at 37°C with 5% CO₂. Cells treated with 0.5% dimethyl sulfoxide were used as a vehicle control (0 μ M). Post-treatment, cells were lysed in radioimmunoprecipitation assay buffer (catalog number 89900; Pierce/Thermo Fisher Scientific, Rockford, IL, USA) and the cell lysates were clarified by centrifugation at 12,000 $\times g$ for 10 min at 4°C. Protein concentrations were determined and the lysates were subjected to 12% sodium dodecyl sulfate polyacrylamide gel electrophoresis. The separated proteins were transferred onto polyvinylidene fluoride membranes (Millipore, Billerica, MA, USA). The membranes were incubated with primary antibodies overnight at 4°C. The primary antibodies included anti-B-cell lymphoma-2 (Bcl-2) antibody (catalog number 2876) and anti-poly(ADP-ribose) polymerase (PARP) rabbit mAb (catalog number 9532) from Cell Signaling Technology, Inc. (Beverly, MA, USA), anti-Beclin-1 antibody (catalog number NB110-87318), anti-LC3B antibody (catalog number NB100-2220), anti-p62/SQSTM1 antibody (catalog number NBP1-42822), and anti-beta-actin antibody (catalog number NB600-501) from Novus Biologicals (Littleton, CO, USA), and anti-ATG-7 (C-term) antibody (catalog number AP1813D) from Abgent (San Diego, CA, USA). The membranes were incubated with alkaline phosphatase-conjugated secondary antibodies (Sigma-Aldrich). Signals were visualized using a chemiluminescence kit (Chemicon), following the manufacturer's protocol. Proteins were quantified by densitometry using ImageJ software.

Statistical analysis

All data are the mean \pm standard error of mean (SEM) of three independent experiments and were analyzed using GraphPad Prism software (GraphPad Software, La Jolla, CA, USA). All data were analyzed using a two-tailed, unpaired Student's *t*-test. A *p*-value of less than 0.05 was considered significant.

Results

Ingredient–lung cancer target network

Our previous study showed that the use of CHM as an adjunctive therapy may reduce the mortality hazard ratio in patients with lung cancer in Taiwan (Li et al., 2018a). CHM network analysis for patients with lung cancer revealed a major cluster that comprised a core CHM, BM, and its combinations. In this cluster, JG and MMDT were important CHMs. To investigate the possible therapeutic mechanism underlying the effects of these CHM products on lung cancer, a network pharmacology approach was employed by searching for CHM product-related natural compounds (Ru et al., 2014; Wu et al., 2019; Zhang et al., 2017).

Ingredients and their targets were obtained from the TCMSP, TCM-MESH, and SymMap databases (BM, Table S2; JG, Table S3, MMDT, Tables S4–S8). Ingredient–target interaction data from the three CHM databases were used to plot the networks for BM, JG, and MMDT using Cytoscape (Fig. S1–S3). In Fig. 1, green diamonds indicate ingredients of BM, JG, and MMDT, whereas yellow marks with red circles are their lung cancer targets. As shown in Fig. 1, BM, JG, and MMDT had 20 natural compounds, each of which targeted at least 20 lung cancer cellular proteins (Fig. 1 and Table 1). Of these, 17 compounds, including ursolic acid, beta-elemene, quercetin, 2-[(3R)-8,8-dimethyl-3,4-dihydro-2H-pyrano[6,5-f]chromen-3-yl]-5-methoxyphenol, beta-sitosterol, licochalcone A, 1-methoxyphaseollidin, baicalein, naringenin, 7-methoxy-2-methyl isoflavone, (L)-alpha-terpineol, luteolin, acacetin, and kaempferol are commercially available (Fig. S4A).

Effects of 17 natural compounds on the proliferation of human lung cancer A549 cells

We investigated the anti-lung cancer effects of these 17 natural compounds identified by network analysis by treating A549 cells with each compound at various concentrations (10, 50, and 100 μM) for 24 h. Cell viability was determined by WST-1 assay (Fig. S4A). Three chemotherapy drugs, cisplatin, paclitaxel, and topotecan, which are used in clinic for the treatment of lung cancer patients (Lyss et al., 2002), were included in the experiments as positive controls. At 100 μM concentration, cisplatin inhibited A549 lung cancer cell growth to 69%, whereas paclitaxel dramatically reduced cell growth to 6%. Topotecan did not significantly reduce A549 cell growth. Three of the 17 natural compounds inhibited cell proliferation, including ursolic acid, 2-[(3R)-8,8-dimethyl-3,4-dihydro-2H-pyrano[6,5-f]chromen-3-yl]-5-methoxyphenol, and licochalcone A. At 100 μM , ursolic acid suppressed A549 cell growth to 38%. At the same concentration, 2-[(3R)-8,8-dimethyl-3,4-dihydro-2H-pyrano[6,5-f]chromen-3-yl]-5-methoxyphenol and licochalcone A inhibited A549 cell growth to 7%. As compared with cisplatin and paclitaxel, ursolic acid, 2-[(3R)-8,8-dimethyl-3,4-dihydro-2H-pyrano[6,5-f]chromen-3-yl]-5-methoxyphenol, and licochalcone A may thus serve as potential candidates for the treatment of lung cancer.

Next we investigated whether the three natural compounds could enhance the inhibition of cell proliferation when combined with cisplatin, paclitaxel, or topotecan by WST-1 assay. The three natural compounds were used at 40 μM to prevent killing too many A549 lung cancer cells. Cells were cultured for 24 h in the presence of cisplatin (0, 50 nM, 50 μM , or 100 μM) and ursolic acid (40 μM), 2-[(3R)-8,8-dimethyl-3,4-dihydro-2H-pyrano[6,5-f]chromen-3-yl]-5-methoxyphenol (40 μM), or licochalcone A (40 μM) (Fig. S4B). Ursolic acid and 2-[(3R)-8,8-dimethyl-3,4-dihydro-2H-pyrano[6,5-f]chromen-3-yl]-5-methoxyphenol promoted the cytotoxicity of cisplatin (100 μM) and further reduced cell growth to 17% and 40%, respectively. Licochalcone A had no additional effect in cisplatin-treated cells. When cells were cultured for 24 h in the presence of paclitaxel (0, 50 nM, 50 μM , or 100 μM) and either of the three natural

compounds at 40 μM , there was no significant additional reduction in these three natural compounds plus paclitaxel-treated cells. When cells were cultured in the presence of topotecan (0, 50 nM, 50 μM , or 100 μM) and of the three natural compounds at 40 μM for 24 h, ursolic acid and 2-[(3R)-8,8-dimethyl-3,4-dihydro-2H-pyrano[6,5-f]chromen-3-yl]-5-methoxyphenol promoted the cytotoxicity of topotecan (50 μM) and further reduced proliferation to 11% and 47%, respectively, whereas licochalcone A had no additional effect in topotecan-treated cells.

Ursolic acid, 2-[(3R)-8,8-dimethyl-3,4-dihydro-2H-pyrano[6,5-f]chromen-3-yl]-5-methoxyphenol, and licochalcone A induce apoptosis in A549 cells

We used Annexin V/PI staining to evaluate whether the three compounds reduced cell proliferation by inducing apoptosis in A549 cells. The apoptotic cell fraction was higher in treated than in non-treated control cells (Fig. 2A). Ursolic acid at 80 μM induced approximately 16% apoptotic cells after 24-h treatment (Fig. 2B), whereas 40 μM of 2-[(3R)-8,8-dimethyl-3,4-dihydro-2H-pyrano[6,5-f]chromen-3-yl]-5-methoxyphenol induced approximately 32% apoptosis after 24 h (Fig. 2B). Treatment of cells with licochalcone A at 40 μM for 24 h resulted in approximately 11% apoptosis (Fig. 2B).

Because they inhibited A549 lung cancer cell proliferation *in vitro*, the three ingredients and their lung cancer targets were subjected to IPA and KEGG signaling pathway analysis, which revealed that the natural compounds may target cellular apoptosis-, anti-apoptosis-, and cell cycle-related proteins. Therefore, we investigated the effects of these compounds on lung cancer cell proliferation.

We examined the expression of cellular proteins involved in programmed cell death control by western blot analysis. Treatment of cells with ursolic acid resulted in a decrease in the levels of anti-apoptotic proteins Bcl-2 and full-length PARP, and increased the level of the apoptotic protein cleaved PARP (Fig. 2C). Bcl-2 protein expression was reduced to 63% in cells treated with 80 μM

ursolic acid (Fig. 2C; $p < 0.0001$). The expression of full-length PARP protein was reduced to 68% (Fig. 2C; $p < 0.0001$) and that of cleaved PARP was increased to 195% in cells treated with 80 μM ursolic acid (Fig. 2C; $p < 0.0001$). Treatment of cells with 2-[(3R)-8,8-dimethyl-3,4-dihydro-2H-pyrano[6,5-f]chromen-3-yl]-5-methoxyphenol resulted in decreases in the expression of Bcl-2 and full-length PARP (Fig. 2D), whereas no difference was observed in the level of cleaved PARP. Bcl-2 protein expression was reduced to 35% in cells treated with 80 μM 2-[(3R)-8,8-dimethyl-3,4-dihydro-2H-pyrano[6,5-f]chromen-3-yl]-5-methoxyphenol (Fig. 2D; $p < 0.0001$), whereas that of full-length PARP was reduced to 79% (Fig. 2D; $p < 0.0001$). Cells treated with licochalcone A showed a decrease in the expression of Bcl-2 and full-length PARP (Fig. 2E), whereas no effect was observed on the level of cleaved PARP protein. Bcl-2 protein expression was reduced to 59% in cells treated with 80 μM licochalcone A (Fig. 2E; $p < 0.0001$). The expression of full-length PARP was reduced to 61% in cells treated with 80 μM licochalcone A (Fig. 2E; $p < 0.0001$). These results suggested that these three natural compounds induced apoptosis through the regulation of apoptotic and anti-apoptotic protein expression in A549 lung cancer cells.

Ursolic acid, 2-[(3R)-8,8-dimethyl-3,4-dihydro-2H-pyrano[6,5-f]chromen-3-yl]-5-methoxyphenol, and licochalcone A induce cell cycle arrest in A549 cells

Cell cycle distribution in A549 cells treated with various concentrations of the three natural compounds was determined by cell cycle assay. The number of cells in G0/G1 phase decreased with increasing concentration (20, 40, and 80 μM , respectively) of each natural compound (Fig. 3B, C, and D). In addition, each natural compound dose-dependently induced increases in the number of cells in S and G2/M phases (Fig. 3B, C, and D). These results suggested that ursolic acid, 2-[(3R)-8,8-dimethyl-3,4-dihydro-2H-pyrano[6,5-f]chromen-3-yl]-5-methoxyphenol, and licochalcone A may induce cell cycle arrest in S and G2/M phases.

Ursolic acid, 2-[(3R)-8,8-dimethyl-3,4-dihydro-2H-pyrano[6,5-f]chromen-3-yl]-5-methoxyphenol, and licochalcone A induce autophagy in A549 cells

Next, we investigated autophagy in A549 cells treated with the three ingredients by examining the expression of proteins involved in autophagy, including Beclin-1, ATG-7, LC3-I, LC3-II, and P62, by western blot analysis. Treatment of cells with ursolic acid resulted in increases in the LC3-II/LC3-I ratio and P62 level (Fig. 4A). The LC3-II/LC3-I ratio was increased to 139% in cells treated with 20 μ M ursolic acid (Fig. 4A; $p < 0.0001$). P62 protein expression was increased to 321% (Fig. 4A; $p < 0.0001$). Treatment of cells with 2-[(3R)-8,8-dimethyl-3,4-dihydro-2H-pyrano[6,5-f]chromen-3-yl]-5-methoxyphenol resulted in a decrease in ATG-7 expression and an increase in the LC3-II/LC3-I ratio (Fig. 4B). ATG-7 protein expression was reduced to 54% in cells treated with 40 μ M 2-[(3R)-8,8-dimethyl-3,4-dihydro-2H-pyrano[6,5-f]chromen-3-yl]-5-methoxyphenol (Fig. 4B; $p < 0.0001$), whereas the LC3-II/LC3-I ratio was increased to 120% in cells treated with 20 μ M 2-[(3R)-8,8-dimethyl-3,4-dihydro-2H-pyrano[6,5-f]chromen-3-yl]-5-methoxyphenol (Fig. 4B; $p < 0.0001$) but decreased with higher concentrations. Cells treated with licochalcone A showed a decrease in ATG-7 expression and increases in the LC3-II/LC3-I ratio and P62 level (Fig. 4C). ATG-7 protein expression was reduced to 64% in cells treated with 40 μ M licochalcone A (Fig. 4C; $p < 0.0001$). The LC3-II/LC3-I ratio was increased to 166% in cells treated with 40 μ M licochalcone A (Fig. 4C; $p < 0.0001$), but decreased with higher concentrations. P62 expression was increased to 121% in cells treated with 40 μ M licochalcone A (Fig. 4C; $p < 0.0001$), but decreased with higher concentrations. These results suggested that these three natural compounds induced autophagy in lung cancer A549 cells.

Discussion

Patients with lung cancer on CHM as adjunctive therapy showed improved cumulative survival (Li et al., 2018a). CHM usage network analysis showed that BM, JG, and MMDT were the major modalities in these patients. In the present study, we systematically explored the compounds of these three CHMs and evaluated their human protein targets. In addition, we investigated the effects of three natural compounds on apoptosis, cell cycle progression, autophagy, and related protein expression in lung cancer cells *in vitro*.

Natural compounds serve as a resource of anticancer agents, and some natural compounds and their chemical derivatives are used in clinical applications (Bailon-Moscoso et al., 2017; Venkata Sairam et al., 2016). There are currently several CHM databases that provide data on herb-related ingredients, ingredient–target interactions, and/or target–disease interactions that allow systemic network pharmacological study of ingredient–target interactions and may help elucidate how CHMs serve as multi-target drugs in modern medicine (Li and Zhang, 2013; Ru et al., 2014; Wu et al., 2019; Zhang et al., 2017). Many CHM targets are involved in pathways associated with tumorigenesis (Guo et al., 2017). The network pharmacological approach has also been applied to unveiling the biological basis of herbal medicine in cancer treatment (Zheng et al., 2018). In this study, we found that there were seven ingredients in BM (*Fritillaria cirrhosa* D. Don, family Liliaceae), which had 44 targets. There were nine ingredients and 130 targets in JG (*Platycodon grandiflorus* (Jacq.) A.DC., family Campanulaceae). However, experimental results showed that neither BM nor JG ingredients exhibited inhibitory effects on lung cancer cell proliferation in this study. For MMDT, hundreds of natural compounds and thousands of human protein targets were found. Three ingredients, ursolic acid, 2-[(3R)-8,8-dimethyl-3,4-dihydro-2H-pyrano[6,5-f]chromen-3-yl]-5-methoxyphenol (also known as glabridin), and licochalcone A, were detected in GC (*Glycyrrhiza uralensis* Fisch., family Leguminosae) (one herb in MMDT) based on their LC retention time and MS ions (Fig. S7A, S7B, and S7C). Experimental results showed that only these three ingredients inhibited A549 lung cancer

cell proliferation *in vitro*. The three ingredients and their lung cancer targets were subjected to IPA and KEGG signaling pathway analysis. The three ingredients had 58 lung cancer targets, 21 and 35 of which were identified by IPA and KEGG pathway analysis, respectively (Table S12). IPA mapped the 21 lung cancer targets to two networks; Network 1_Neurological Disease, Cancer, Organismal and Abnormalities and Network 2_ Cellular Assembly and Organization, Cellular Function and Maintenance, Cell Death and Survival (Fig. S5 and Table S12). KEGG analysis revealed a network specialized in pathways in cancer, and possible compound-targeted lung cancer proteins were highlighted with a yellow mark (Fig. S6 and Table S12). These pathway analyses suggested that the natural compounds may target apoptosis-, anti-apoptosis-, and cell cycle-related proteins. Therefore, we investigated the effects of these compounds on lung cancer cell proliferation.

Ursolic acid is known to inhibit the proliferation of various cancer cells, including human colon carcinoma (Wang et al., 2013b), prostate cancer (Meng et al., 2015), liver cancer (Liu et al., 2017), breast cancer (Li et al., 2018b), melanoma (Oprean et al., 2018), leukemia (Li et al., 2013), and lung cancer (Mendes et al., 2016; Yuan et al., 2015) cells. In agreement with previous studies (Mendes et al., 2016; Yuan et al., 2015), we found that ursolic acid suppressed A549 lung cancer cell proliferation by inducing apoptosis, cell cycle arrest, and autophagy. We observed the accumulation of apoptotic cells in ursolic acid-treated cells, with concomitant decreases in anti-apoptotic proteins Bcl-2 and full-length PARP, and an increase in the apoptotic protein cleaved PARP (Yuan et al., 2015). The major difference between our study and the study by Yuan et al. (2015) was that the cell fraction in the G0/G1 phase decreased after treatment with ursolic acid in a dose-dependent manner, whereas the number of cells in S and G2/M phases increased, suggesting that ursolic acid may induce cell cycle arrest in the S and G2/M phases, not in the G0/G1 phase (Yuan et al., 2015).

The compound 2-[(3R)-8,8-dimethyl-3,4-dihydro-2H-pyran[6,5-f]chromen-3-yl]-5-methoxyphenol is also known as glabridin and has been shown to inhibit the proliferation of various cancer cells, including human

liver cancer (Hsieh et al., 2016; Wang et al., 2016), breast cancer (Tamir et al., 2000), and leukemia (Huang et al., 2014) cells. We found that 2-[(3R)-8,8-dimethyl-3,4-dihydro-2H-pyrano[6,5-f]chromen-3-yl]-5-methoxyphenol inhibited A549 cell proliferation by inducing apoptosis, cell cycle arrest, and autophagy. The number of apoptotic cells increased after 2-[(3R)-8,8-dimethyl-3,4-dihydro-2H-pyrano[6,5-f]chromen-3-yl]-5-methoxyphenol treatment and the expression of Bcl-2 and full-length PARP decreased. Furthermore, the number of cells in G0/G1 phase decreased and the number of cells in S and G2/M phases increased after treatment with this compound in a dose-dependent manner, suggestive of its ability to induce cell cycle arrest in S and G2/M phases. Glabridin has been shown to inhibit lung cancer cell migration, invasion, and angiogenesis by suppressing FAK/Rho signaling (Tsai et al., 2011). These results suggest that 2-[(3R)-8,8-dimethyl-3,4-dihydro-2H-pyrano[6,5-f]chromen-3-yl]-5-methoxyphenol may act as a potential anti-lung cancer agent by inducing apoptosis and cell cycle arrest and inhibiting migration, invasion, and angiogenesis of lung cancer cells.

Licochalcone A inhibits the proliferation of human colon (Lee et al., 2008), prostate (Fu et al., 2004; Yo et al., 2009), liver (Niu et al., 2018; Wang et al., 2018), breast (Bortolotto et al., 2017; Kang et al., 2017; Xue et al., 2018), and lung (Chen et al., 2018; Qiu et al., 2017; Tang et al., 2016) cancer cells. In agreement with previous studies (Chen et al., 2018; Qiu et al., 2017; Tang et al., 2016), we found that licochalcone A inhibited A549 cell proliferation by inducing apoptosis, cell cycle arrest, and autophagy. Apoptotic cells accumulated after licochalcone A treatment and Bcl-2 and full-length PARP levels decreased (Qiu et al., 2017). A549 cells treated with licochalcone A were arrested in G2/M phase (Qiu et al., 2017). We observed that licochalcone A also induced autophagy by enhancing the LC3-II/LC3-I ratio and P62 expression. Our results were in agreement with those of Tang et al. (2016), who reported on A549 lung cancer cells treated with licochalcone A undergoing apoptosis and autophagy via increased LC3-II expression.

Conclusions

BM, JG, and MMDT are important CHMs prescribed for patients with lung cancer. Experimental results showed that three of their ingredients, *i.e.*, ursolic acid, 2-[(3R)-8,8-dimethyl-3,4-dihydro-2H-pyrano[6,5-f]chromen-3-yl]-5-methoxyphenol, and licochalcone A, inhibit A549 lung cancer cell proliferation. IPA and KEGG analysis of these three ingredients and their corresponding lung cancer targets revealed their potential effects on cell apoptosis and cycle progression. *In-vitro* accumulation of apoptotic cells after treatment with these three ingredients was related to their modulatory effects on apoptotic and anti-apoptotic protein expression. Cell cycle was arrested in S and G2/M phases and autophagy was induced in A549 cells treated with these ingredients. Therefore, these CHM-related natural compounds with anti-lung cancer properties may be useful in adjunctive therapy in patients with lung cancer. Further studies are warranted to optimize the safety and efficacy of CHMs.

Funding

This study was supported by grants from China Medical University [CMU107-S-13 and CMU107-S-15], China Medical University Hospital [DMR-107-042, DMR-108-113, DMR-108-114, and DMR-108-118], and the National Science Council, the Ministry of Science and Technology, Taiwan [MOST 105-2314-B-039-037-MY3, and MOST 106-2320-B-039-017-MY3].

Acknowledgements

This study was based entirely on data from the National Health Insurance Research Database provided by the Bureau of National Health Insurance, Department of Health and managed by the National Health Research Institutes. The interpretation and conclusions contained herein do not represent those of the National Health Insurance Administration, Department of Health, or National Health Research Institutes. We thank Professor Jianxin Chen for providing his SymMap database.

We thank Drs. Ruey-Hwang Chou, Chih-Ho Lai, Cherry Yin-Yi Chang, Kuan-Teh Jeang, and Willy W.L. Hong for technical help and suggestions.

Conflict of interest

The authors have no conflicts of interest to disclose.

References

- Bailon-Moscoso, N., Cevallos-Solorzano, G., Romero-Benavides, J.C., Orellana, M.I., (2017). Natural Compounds as Modulators of Cell Cycle Arrest: Application for Anticancer Chemotherapies. *Curr Genomics* 18, 106-131.
- Bortolotto, L.F., Barbosa, F.R., Silva, G., Bitencourt, T.A., Belebony, R.O., Baek, S.J., Marins, M., Fachin, A.L., (2017). Cytotoxicity of trans-chalcone and licochalcone A against breast cancer cells is due to apoptosis induction and cell cycle arrest. *Biomed Pharmacother* 85, 425-433.
- Chen, G., Ma, Y., Jiang, Z., Feng, Y., Han, Y., Tang, Y., Zhang, J., Ni, H., Li, X., Li, N., (2018). Lico A Causes ER Stress and Apoptosis via Up-Regulating miR-144-3p in Human Lung Cancer Cell Line H292. *Front Pharmacol* 9, 837.
- Chiang, C.J., Lo, W.C., Yang, Y.W., You, S.L., Chen, C.J., Lai, M.S., (2016). Incidence and survival of adult cancer patients in Taiwan, 2002-2012. *J Formos Med Assoc* 115, 1076-1088.
- Fu, Y., Hsieh, T.C., Guo, J., Kunicki, J., Lee, M.Y., Darzynkiewicz, Z., Wu, J.M., (2004). Licochalcone-A, a novel flavonoid isolated from licorice root (*Glycyrrhiza glabra*), causes G2 and late-G1 arrests in androgen-independent PC-3 prostate cancer cells. *Biochem Biophys Res Commun* 322, 263-270.
- Guo, Y., Nie, Q., MacLean, A.L., Li, Y., Lei, J., Li, S., (2017). Multiscale Modeling of Inflammation-Induced Tumorigenesis Reveals Competing Oncogenic and Oncoprotective Roles for Inflammation. *Cancer Res* 77, 6429-6441.
- Hsieh, M.J., Chen, M.K., Chen, C.J., Hsieh, M.C., Lo, Y.S., Chuang, Y.C., Chiou, H.L., Yang, S.F., (2016). Glabridin induces apoptosis and autophagy through JNK1/2 pathway in human hepatoma cells. *Phytomedicine* 23, 359-366.
- Hsu, W.L., Tsai, Y.T., Wu, C.T., Lai, J.N., (2015). The Prescription Pattern of Chinese Herbal Products Containing Ginseng among Tamoxifen-Treated Female Breast Cancer Survivors in Taiwan: A Population-Based Study. *Evid Based Complement Alternat Med* 2015, 385204.
- Huang, H.L., Hsieh, M.J., Chien, M.H., Chen, H.Y., Yang, S.F., Hsiao, P.C., (2014). Glabridin mediate caspases activation and induces apoptosis through JNK1/2 and p38 MAPK pathway in human promyelocytic leukemia cells. *PLoS One* 9, e98943.

- Huang, T.P., Liu, P.H., Lien, A.S., Yang, S.L., Chang, H.H., Yen, H.R., (2013). Characteristics of traditional Chinese medicine use in children with asthma: a nationwide population-based study. *Allergy* 68, 1610-1613.
- Kang, T.H., Seo, J.H., Oh, H., Yoon, G., Chae, J.I., Shim, J.H., (2017). Licochalcone A Suppresses Specificity Protein 1 as a Novel Target in Human Breast Cancer Cells. *J Cell Biochem* 118, 4652-4663.
- Lee, C.K., Son, S.H., Park, K.K., Park, J.H., Lim, S.S., Kim, S.H., Chung, W.Y., (2008). Licochalcone A inhibits the growth of colon carcinoma and attenuates cisplatin-induced toxicity without a loss of chemotherapeutic efficacy in mice. *Basic Clin Pharmacol Toxicol* 103, 48-54.
- Lee, Y.C., Huang, Y.T., Tsai, Y.W., Huang, S.M., Kuo, K.N., McKee, M., Nolte, E., (2010). The impact of universal National Health Insurance on population health: the experience of Taiwan. *BMC Health Serv Res* 10, 225.
- Li, G., Zhou, T., Liu, L., Chen, J., Zhao, Z., Peng, Y., Li, P., Gao, N., (2013). Ezrin dephosphorylation/downregulation contributes to ursolic acid-mediated cell death in human leukemia cells. *Blood Cancer J* 3, e108.
- Li, S., Zhang, B., (2013). Traditional Chinese medicine network pharmacology: theory, methodology and application. *Chin J Nat Med* 11, 110-120.
- Li, T.M., Yu, Y.H., Tsai, F.J., Cheng, C.F., Wu, Y.C., Ho, T.J., Liu, X., Tsang, H., Lin, T.H., Liao, C.C., Huang, S.M., Li, J.P., Lin, J.C., Lin, C.C., Liang, W.M., Lin, Y.J., (2018a). Characteristics of Chinese herbal medicine usage and its effect on survival of lung cancer patients in Taiwan. *J Ethnopharmacol* 213, 92-100.
- Li, W., Zhang, H., Nie, M., Wang, W., Liu, Z., Chen, C., Chen, H., Liu, R., Baloch, Z., Ma, K., (2018b). A novel synthetic ursolic acid derivative inhibits growth and induces apoptosis in breast cancer cell lines. *Oncol Lett* 15, 2323-2329.
- Liang, C.Z., Zhang, J.K., Shi, Z., Liu, B., Shen, C.Q., Tao, H.M., (2012). Matrine induces caspase-dependent apoptosis in human osteosarcoma cells in vitro and in vivo through the upregulation of Bax and Fas/FasL and downregulation of Bcl-2. *Cancer Chemother Pharmacol* 69, 317-331.
- Liu, T., Ma, H., Shi, W., Duan, J., Wang, Y., Zhang, C., Li, C., Lin, J., Li, S., Lv, J., Lin, L., (2017). Inhibition of STAT3 signaling pathway by ursolic acid suppresses growth of hepatocellular carcinoma. *Int J Oncol* 51, 555-562.
- Lu, P., (2016). Inhibitory effects of hyperoside on lung cancer by inducing apoptosis and suppressing inflammatory response via caspase-3 and NF-kappaB signaling pathway. *Biomed Pharmacother* 82, 216-225.
- Lyss, A.P., Herndon, J.E., 2nd, Lynch, T.J., Jr., Turrisi, A.T., Watson, D.M., Grethlein, S.J., Green, M.R., (2002). Novel doublets in extensive-stage small-cell lung cancer: a randomized phase II study of topotecan plus cisplatin or paclitaxel (CALGB 9430). *Clin Lung Cancer* 3,

205-210; discussion 211-202.

- Mendes, V.I.S., Bartholomeusz, G.A., Ayres, M., Gandhi, V., Salvador, J.A.R., (2016). Synthesis and cytotoxic activity of novel A-ring cleaved ursolic acid derivatives in human non-small cell lung cancer cells. *Eur J Med Chem* 123, 317-331.
- Meng, Y., Lin, Z.M., Ge, N., Zhang, D.L., Huang, J., Kong, F., (2015). Ursolic Acid Induces Apoptosis of Prostate Cancer Cells via the PI3K/Akt/mTOR Pathway. *Am J Chin Med* 43, 1471-1486.
- Niu, H., Wang, J., Li, H., He, P., (2011). Rapamycin potentiates cytotoxicity by docetaxel possibly through downregulation of Survivin in lung cancer cells. *J Exp Clin Cancer Res* 30, 28.
- Niu, Q., Zhao, W., Wang, J., Li, C., Yan, T., Lv, W., Wang, G., Duan, W., Zhang, T., Wang, K., Zhou, D., (2018). LicA induces autophagy through ULK1/Atg13 and ROS pathway in human hepatocellular carcinoma cells. *Int J Mol Med* 41, 2601-2608.
- Oprean, C., Ivan, A., Bojin, F., Cristea, M., Soica, C., Draghia, L., Caunii, A., Paunescu, V., Tatu, C., (2018). Selective in vitro anti-melanoma activity of ursolic and oleanolic acids. *Toxicol Mech Methods* 28, 148-156.
- Qiu, C., Zhang, T., Zhang, W., Zhou, L., Yu, B., Wang, W., Yang, Z., Liu, Z., Zou, P., Liang, G., (2017). Licochalcone A Inhibits the Proliferation of Human Lung Cancer Cell Lines A549 and H460 by Inducing G2/M Cell Cycle Arrest and ER Stress. *Int J Mol Sci* 18.
- Ru, J., Li, P., Wang, J., Zhou, W., Li, B., Huang, C., Li, P., Guo, Z., Tao, W., Yang, Y., Xu, X., Li, Y., Wang, Y., Yang, L., (2014). TCMSP: a database of systems pharmacology for drug discovery from herbal medicines. *J Cheminform* 6, 13.
- Shannon, P., Markiel, A., Ozier, O., Baliga, N.S., Wang, J.T., Ramage, D., Amin, N., Schwikowski, B., Ideker, T., (2003). Cytoscape: a software environment for integrated models of biomolecular interaction networks. *Genome Res* 13, 2498-2504.
- Shi, S., Tan, P., Yan, B., Gao, R., Zhao, J., Wang, J., Guo, J., Li, N., Ma, Z., (2016). ER stress and autophagy are involved in the apoptosis induced by cisplatin in human lung cancer cells. *Oncol Rep* 35, 2606-2614.
- Tamir, S., Eizenberg, M., Somjen, D., Stern, N., Shelach, R., Kaye, A., Vaya, J., (2000). Estrogenic and antiproliferative properties of glabridin from licorice in human breast cancer cells. *Cancer Res* 60, 5704-5709.
- Tang, Z.H., Chen, X., Wang, Z.Y., Chai, K., Wang, Y.F., Xu, X.H., Wang, X.W., Lu, J.H., Wang, Y.T., Chen, X.P., Lu, J.J., (2016). Induction of C/EBP homologous protein-mediated apoptosis and autophagy by licochalcone A in non-small cell lung cancer cells. *Sci Rep* 6, 26241.
- Tsai, F.J., Ho, T.J., Cheng, C.F., Liu, X., Tsang, H., Lin, T.H., Liao, C.C., Huang, S.M., Li, J.P., Lin, C.W., Lin, J.G., Lin, J.C., Lin, C.C., Liang, W.M., Lin, Y.J., (2017). Effect of Chinese herbal medicine on stroke patients with type 2 diabetes. *J Ethnopharmacol* 200, 31-44.
- Tsai, Y.M., Yang, C.J., Hsu, Y.L., Wu, L.Y., Tsai, Y.C., Hung, J.Y., Lien, C.T., Huang, M.S., Kuo, P.L., (2011). Glabridin inhibits migration, invasion, and angiogenesis of human non-small cell

- lung cancer A549 cells by inhibiting the FAK/rho signaling pathway. *Integr Cancer Ther* 10, 341-349.
- Venkata Sairam, K., Gurupadayya, B.M., Chandan, R.S., Nagesha, D.K., Vishwanathan, B., (2016). A Review on Chemical Profile of Coumarins and their Therapeutic Role in the Treatment of Cancer. *Curr Drug Deliv* 13, 186-201.
- Wang, B.Y., Huang, J.Y., Cheng, C.Y., Lin, C.H., Ko, J., Liaw, Y.P., (2013a). Lung cancer and prognosis in taiwan: a population-based cancer registry. *J Thorac Oncol* 8, 1128-1135.
- Wang, J., Zhang, Y.S., Thakur, K., Hussain, S.S., Zhang, J.G., Xiao, G.R., Wei, Z.J., (2018). Licochalcone A from licorice root, an inhibitor of human hepatoma cell growth via induction of cell apoptosis and cell cycle arrest. *Food Chem Toxicol* 120, 407-417.
- Wang, W., Zhao, C., Jou, D., Lu, J., Zhang, C., Lin, L., Lin, J., (2013b). Ursolic acid inhibits the growth of colon cancer-initiating cells by targeting STAT3. *Anticancer Res* 33, 4279-4284.
- Wang, Z., Luo, S., Wan, Z., Chen, C., Zhang, X., Li, B., Huang, G., Chen, L., He, Z., Huang, Z., (2016). Glabridin arrests cell cycle and inhibits proliferation of hepatocellular carcinoma by suppressing braf/MEK signaling pathway. *Tumour Biol* 37, 5837-5846.
- Wu, Y., Zhang, F., Yang, K., Fang, S., Bu, D., Li, H., Sun, L., Hu, H., Gao, K., Wang, W., Zhou, X., Zhao, Y., Chen, J., (2019). SymMap: an integrative database of traditional Chinese medicine enhanced by symptom mapping. *Nucleic Acids Res* 47, D1110-D1117.
- Xue, L., Zhang, W.J., Fan, Q.X., Wang, L.X., (2018). Licochalcone A inhibits PI3K/Akt/mTOR signaling pathway activation and promotes autophagy in breast cancer cells. *Oncol Lett* 15, 1869-1873.
- Yo, Y.T., Shieh, G.S., Hsu, K.F., Wu, C.L., Shiau, A.L., (2009). Licorice and licochalcone-A induce autophagy in LNCaP prostate cancer cells by suppression of Bcl-2 expression and the mTOR pathway. *J Agric Food Chem* 57, 8266-8273.
- Yuan, Y., Gao, Y., Song, G., Lin, S., (2015). Ursolic acid and oleanolic acid from *Eriobotrya fragrans* inhibited the viability of A549 cells. *Nat Prod Commun* 10, 239-242.
- Zhang, R.Z., Yu, S.J., Bai, H., Ning, K., (2017). TCM-Mesh: The database and analytical system for network pharmacology analysis for TCM preparations. *Sci Rep* 7, 2821.
- Zhang, S., Zhang, Y., Zhuang, Y., Wang, J., Ye, J., Zhang, S., Wu, J., Yu, K., Han, Y., (2012). Matrine induces apoptosis in human acute myeloid leukemia cells via the mitochondrial pathway and Akt inactivation. *PLoS One* 7, e46853.
- Zheng, J., Wu, M., Wang, H., Li, S., Wang, X., Li, Y., Wang, D., Li, S., (2018). Network Pharmacology to Unveil the Biological Basis of Health-Strengthening Herbal Medicine in Cancer Treatment. *Cancers (Basel)* 10.
- Zhong, L.R., Chen, X., Wei, K.M., (2013). Radix tetrastigma hemsleyani flavone induces apoptosis in human lung carcinoma a549 cells by modulating the MAPK pathway. *Asian Pac J Cancer Prev* 14, 5983-5987.

Fig. 2

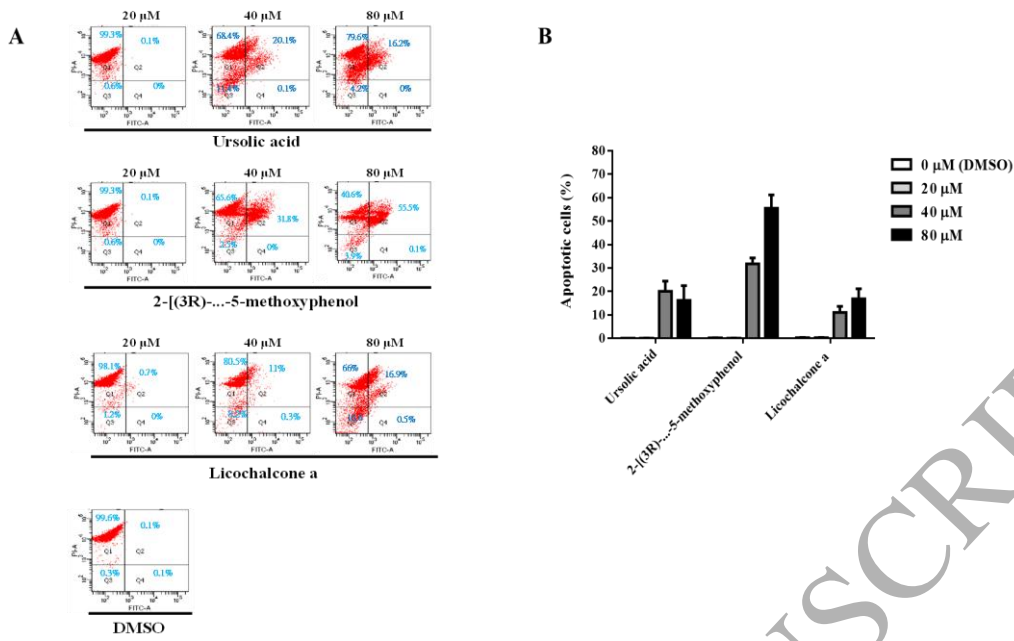


Fig. 2

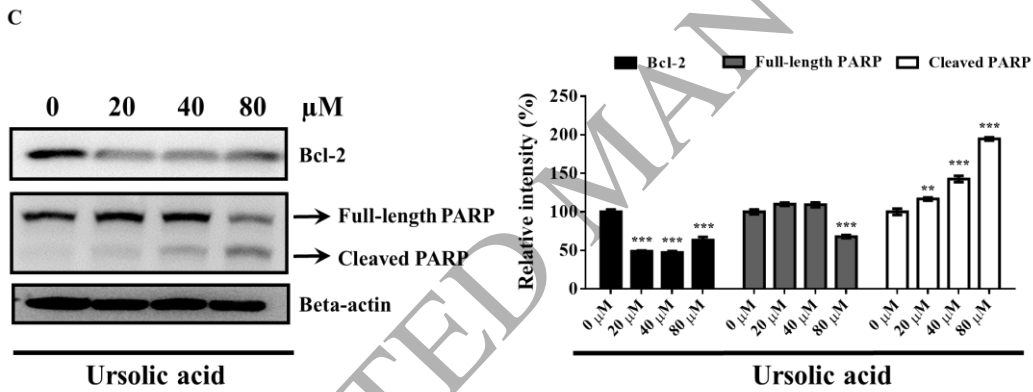


Fig. 2

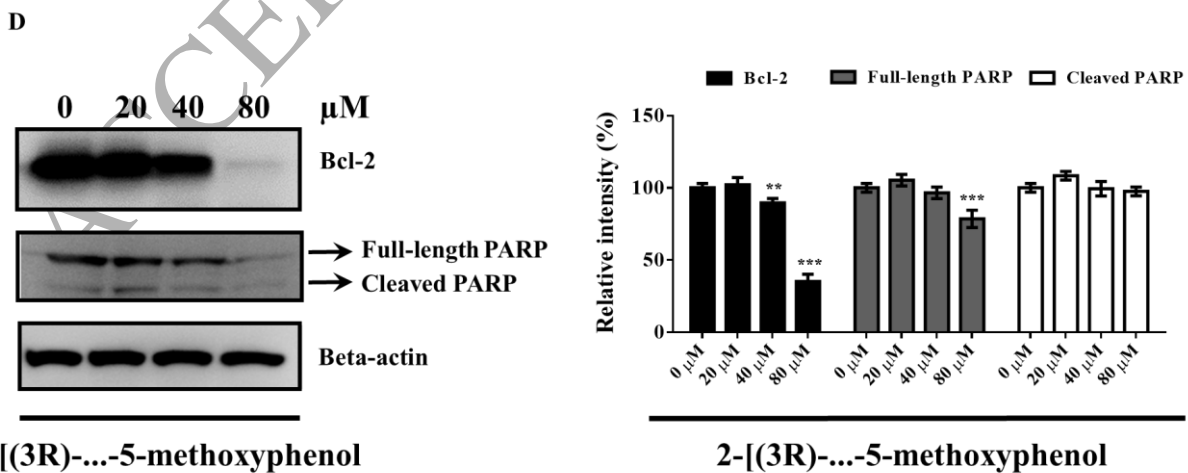


Fig. 2

E

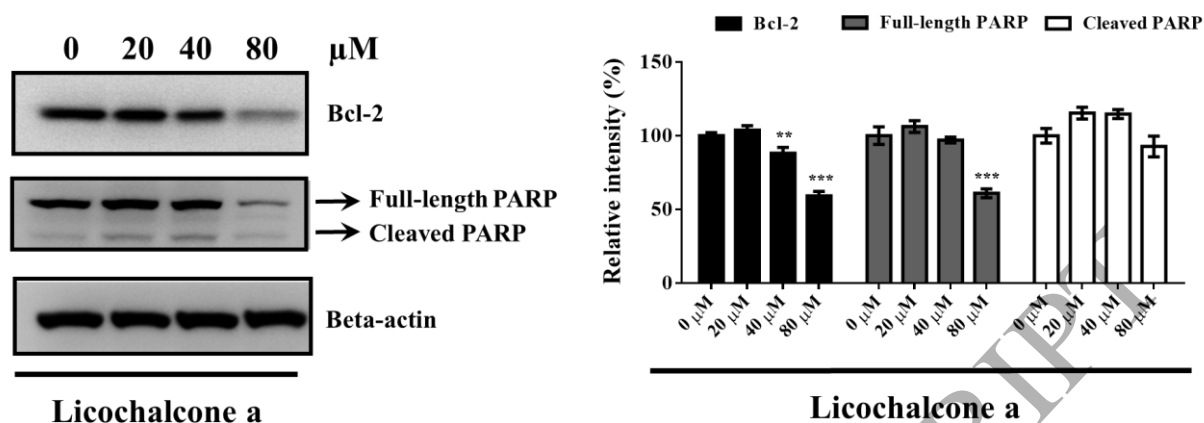


Fig. 2. Detection of apoptosis induced by ursolic acid, 2-[(3R)-8,8-dimethyl-3,4-dihydro-2H-pyrano[6,5-f]chromen-3-yl]-5-methoxyphenol, and licochalcone A by flow cytometry. (A) Apoptosis was evaluated by Annexin V-FITC/PI dual staining assay. Numbers of Annexin V-FITC-positive and PI-positive cells were determined by flow cytometry. Quadrant 1 (Q1): necrotic cells; quadrant 2 (Q2): late-apoptotic cells; quadrant 3 (Q3): viable cells; quadrant 4 (Q4): early apoptotic cells. (B) Apoptotic cells were calculated as the sum of the percentages in the Q2 and Q4 areas. Each concentration was assayed in quadruplicate and data are the mean of three independent experiments. (C) Western blot analysis of Bcl-2, full-length PARP, and cleaved PARP protein expressions in ursolic acid treated A549 cells after 24 hours of exposure. (D) Western blot analysis of Bcl-2, full-length PARP, and cleaved PARP protein expression in A549 cells exposed to 2-[(3R)-8,8-dimethyl-3,4-dihydro-2H-pyrano[6,5-f]chromen-3-yl]-5-methoxyphenol) for 24 h. (E) Western blot analysis of Bcl-2, full-length PARP, and cleaved PARP protein expression in A549 cells exposed to licochalcone A for 24 h. Proteins were quantified by densitometry using ImageJ software.

Fig. 3

A

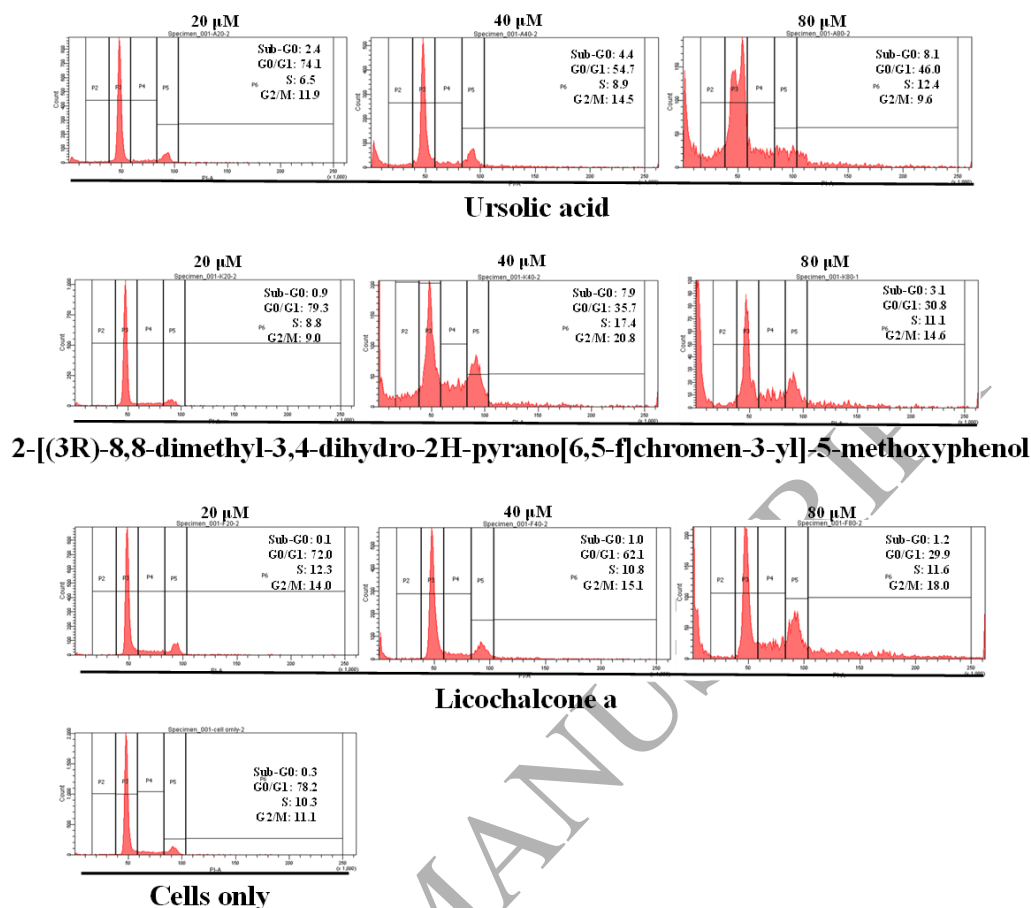


Fig. 3

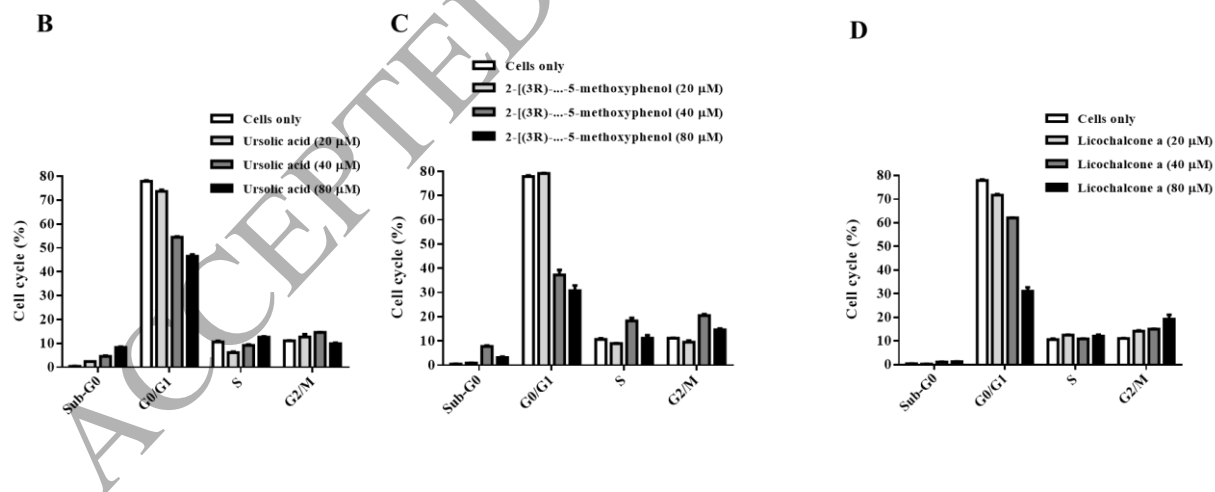


Fig. 3. Detection of cell cycle distribution induced by ursolic acid, 2-[(3R)-8,8-dimethyl-3,4-dihydro-2H-pyrano[6,5-f]chromen-3-yl]-5-methoxyphenol, and licochalcone A by flow cytometry. (A) Cell cycle distribution was evaluated by propidium iodide staining and flow cytometry. (B) Percentages of cells in different phases of the cell cycle upon

treatment with ursolic acid (20, 40, and 80 μ M, respectively). (C) Percentages of cells in different phases of the cell cycle upon treatment with 2-[(3R)-8,8-dimethyl-3,4-dihydro-2H-pyrano[6,5-f]chromen-3-yl]-5-methoxyphenol (20, 40, and 80 μ M, respectively) presented as bar diagram. (D) Percentage of cells in different phases of the cell cycle treatment with licochalcone A (20, 40, and 80 μ M, respectively) presented as bar diagram.

Fig. 4

A

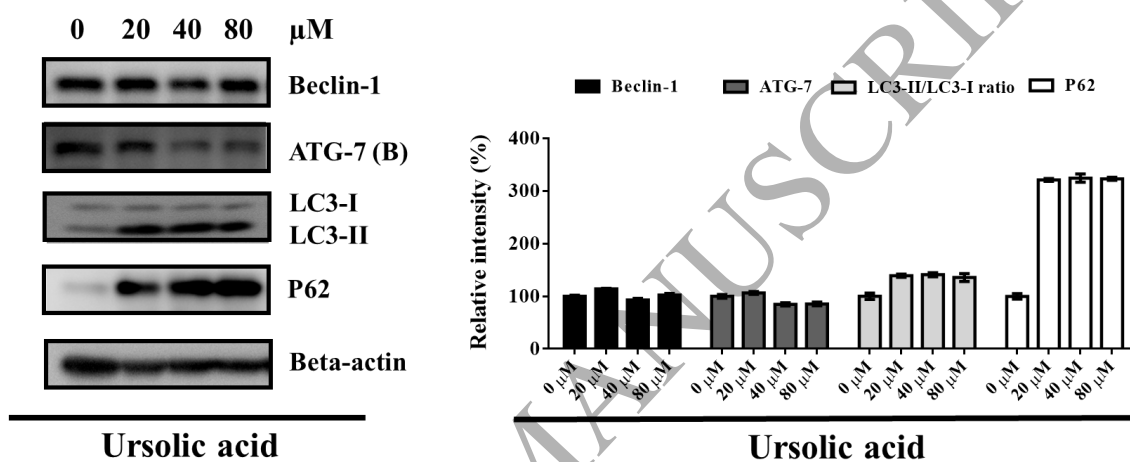


Fig. 4

B

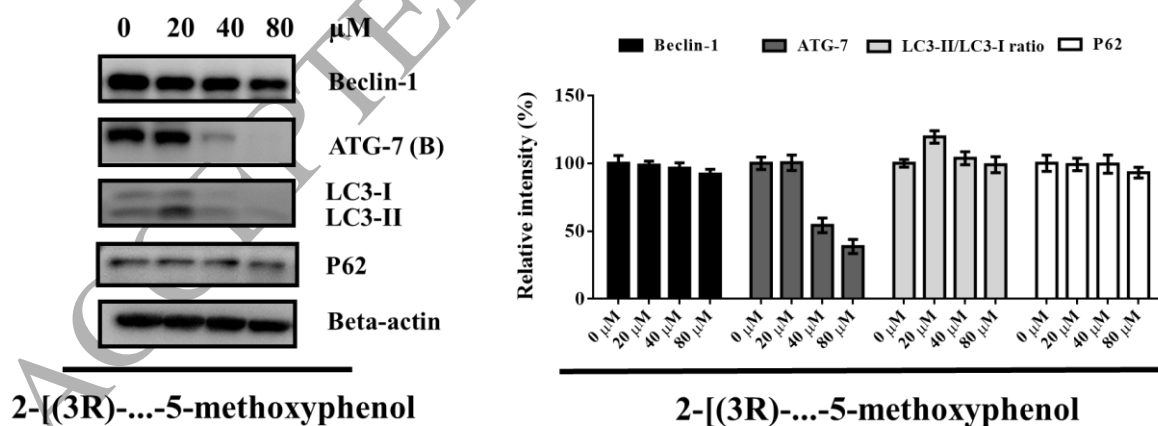


Fig. 4

C

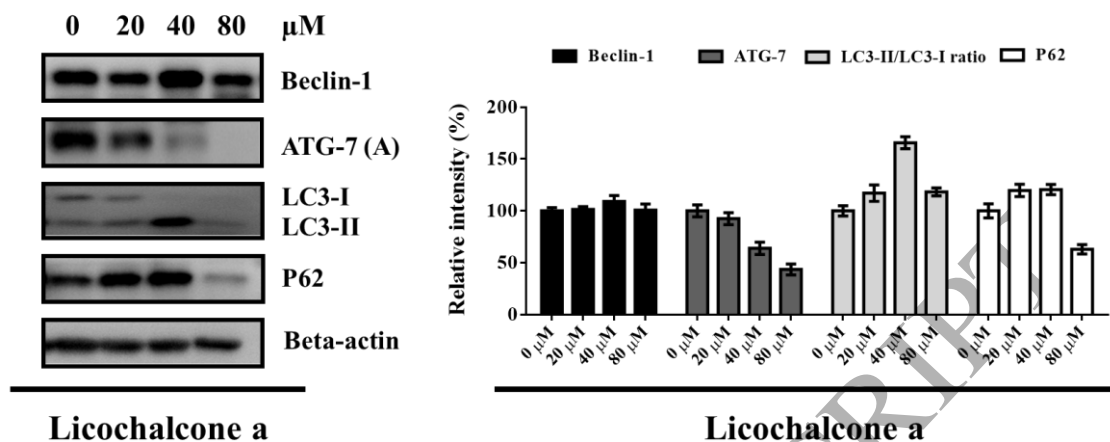


Fig. 4. Detection of autophagy induced by ursolic acid, 2-[(3R)-8,8-dimethyl-3,4-dihydro-2H-pyrano[6,5-f]chromen-3-yl]-5-methoxyphenol, and licochalcone A. (A) Western blot analysis of Beclin-1, ATG-7, LC3-I, LC3-II, and P62 protein expression in A549 cells treated with ursolic acid for 24 h. (B) Western blot analysis of Beclin-1, ATG-7, LC3-I, LC3-II, and P62 protein expression in A549 cells treated with 2-[(3R)-8,8-dimethyl-3,4-dihydro-2H-pyrano[6,5-f]chromen-3-yl]-5-methoxyphenol for 24 h. (C) Western blot analysis of Beclin-1, ATG-7, LC3-I, LC3-II, and P62 protein expression in A549 cells treated with licochalcone A for 24 h. Proteins were quantified by densitometry using ImageJ software.

Table 1. Natural compounds in Chinese herbal products (BM, JG, and MMDT) that targeting at least 20 lung cancer genes from each natural compound

No	Natural compounds (Ingredients)	Multiple CHM databases			Chinese herbal medicine					
		TCM SP	TCM -MES H	SymMap	Bei-Mu (BM)	Jie-Ge (JG)	Mai-Men-Dong-Tang (MMDT)			
							Ren-Shen (RS)	Da-Zao (DZ)	Ban-Xia (BX)	Gan-Cao (GC)
1	Ursolic Acid	v		v			v		v	
2	Beta-Elemene	v	v	v			v	v		
3	Quercetin	v		v			v	v	v	v
4	2-[(3r)-8,8-Dimethyl-3,4-Dihydro-2h-Pyran[6,5-F]chromen-3-Yl]-5-Methoxyphenol	v		v					v	
5	Beta-Sitosterol	v		v	v		v	v		v
6	Licochalcone A	v	v	v					v	
7	1-Methoxyphaseollidin	v		v					v	
8	Baicalein	v		v				v		
9	Naringenin	v		v		v			v	
10	7-Methoxy-2-Methyl Isoflavone	v		v					v	v
11	(L)-Alpha-Terpineol	v		v					v	
12	Luteolin	v		v		v				
13	Acacetin	v		v		v				
14	Kaempferol	v		v			v		v	
1	GLY	v		v			v	v		

5									
1	Castanin	v		v					v
6									
1	3'-Methoxyglabridin	v	v	v					v
7									
1	Palmitic Acid	v		v	v	v	v	v	v
8									
1	Berberine	v	v	v			v		
9									
2	Formononetin	v	v	v					v
0									

Multiple Chinese herbal medicine (CHM) databases include TCMSP, TCM-MESH, and SymMap databases (Table S1).

TCMSP database is located at <http://lsp.nwu.edu.cn/> (Update date: May, 2014).

TCM -MESH database is located at <http://mesh.tcm.microbioinformatics.org/> (Update date: April, 2017).

SymMap database is located at <http://www.symmap.org/search/> (Update date: October, 2018).

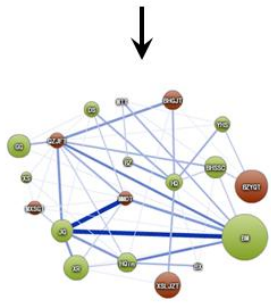
These natural compounds are from Chinese herbal medicine (BM, JG, and MMDT).

Bei-Mu (BM) is composed of *Fritillaria cirrhosa* D.Don, family Liliaceae.

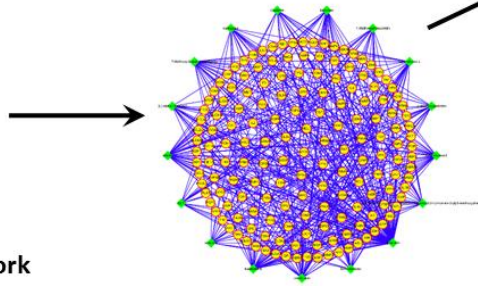
Jie-Geng (JG) is composed of *Platycodon grandiflorus* (Jacq.) A.DC., family Campanulaceae.

For Mai-Men-Dong-Tang (MMDT), there are 5 single herbs used in this study. Ren-Shen (RS) is composed of *Panax ginseng* C.A.Mey., family Araliaceae. Da-Zao (DZ) is composed of *Ziziphus jujuba* Mill., family Rhamnaceae. Ban-Xia (BX) is composed of *Pinellia ternata* (Thumb.) Makino, family Araceae. Gan-Cao (GC) is composed of *Glycyrrhiza uralensis* Fisch., family Leguminosae. Tian-Dong (TD) is composed of *Asparagus cochinchinensis* (Lour.) Merr., family Liliaceae.

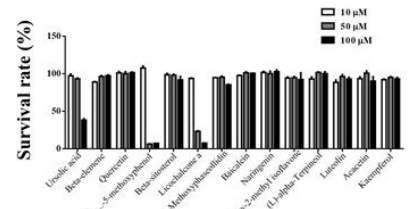
Graphic abstract



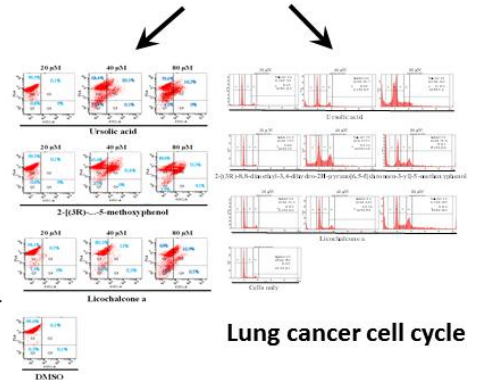
Chinese herbal medicine network of lung cancer patients with better survival



Chinese herbal medicine related Natural compounds-lung cancer cellular protein network



Effects of 14 natural compounds on the cell proliferation of human lung cancer A549 cells



Lung cancer cell apoptosis